Korean J. of Chem. Eng., **7**(1) (1990) *61-68*

A STUDY ON ION EXCHANGE MECHANISMS OF ZEOLITE NaA CRYSTALLITES

Jeikwon MOON and Hanju LEE

Department of Chemical Engineering, Yonsei University, Seoul, Korea

(Received 27 June 1989 • accepted 18 September 1989)

Abstract—The mechanism of Ca^{2+} ion exchange in zeolite NaA powders were studied with varying its crystal size. It was reasoned that the rate of ion exchange at corners and edges of a crystal would be faster than that at the center portion of each crystal face. Therefore, as the degree of ion exchange advances, the front of ion exchange will loose its sharp edges and approaches to a near spherical shape. To take into account of this phenomenon in the analysis of experimental ion exchange rates, rate equations for sphere and cube were combined together in the following form, which may be called as the transition model.

$$f_T(\phi) = \frac{F(\phi)}{\ln \phi} = [1 - g(\theta)]\, f_c(\phi) + g(\theta) f_s(\phi)$$

The transition time function, $g(\theta)$, was assumed to be expressed by $g(\theta) = \alpha\theta^{\beta}$ and the constants were found to be $\alpha = 2.79$, $\beta = 0.43$ in this experiment. Using the transition model equation, the ion exchange rate of zeolite NaA powders would be represented better than either by the spherical or the cubic model alone.

INTRODUCTION

Zeolite NaA powder is widely used as the builder in synthetic detergent formulations replacing the conventional TSPP (tetrasodium pyrophosphate) which is the undesirable cause of eutrophication. Zeolite NaA powder, to be effective as a detergent builder, should have a fast rate of Ca^{2+}/Mg^{2+} ion exchange. Until now the ion exchange rate of zeolite A powders have been analysed by the spherical model, assuming the zeolite crystals to be spherical in shape although it actually has a cubic structure [1,2]. However, because of its cubic shape, the spherical model was found to be unsatisfactory in analysing the experimental data. Therefore, a cubic model was developed and applied in analysis of ion exchange data of a zeolite NaA powder, but showed also a limited success.

In this paper, therefore, the transition model which combines the two simple models, i.e. the cubic and the spherical, was developed and was applied in describing the ion exchange rate of zeolite NaA powders.

ION EXCHANGE MODELS

The conventional model for ion exchange of fine powder dispersed in a finite volume of ionic solution has been based on a spherical model. Based on the same approach as the spherical model, a cubic model could be derived for zeolite NaA powders which has cubic structure. Zeolite NaA powder, however, looses its cubic characteristic as the degree of ion exchange advances, because the corners and edges of cubic crystals have higher ion exchange rate than the other part of cubic crystal. The transition model was developed to accommodate this characteristics by combining the spherical and the cubic models.

1. The spherical model

This model is based on the diffusion equation by Crank for an irreversible adsorption on a spherical particle [3,5]. Digiano and Weber applied the equation onto a batch adsorption of organic compounds on activated carbon granules in a finite volume of the organic solution, and obtained the following rate equation for spherical particles [4],

$$\frac{F(\phi)}{\ln \phi} = \frac{D}{k_f r} + \frac{3wDt}{r^2 \rho_p \ln \phi} \tag{1}$$

where ϕ is a dimensionless concentration, C_t/C_{to}, and $F(\phi)$ is a function of ϕ which is related to the degree of adsorption and can be obtained from experimental data. By plotting $F(\phi)/\ln \phi$ vs. $wt/r^2\rho_p \ln \phi$, the effective pore diffusivity, D, and the film mass transfer coefficient, k_f, could be obtained from the slope and the intercept if the plot is in a linear form.

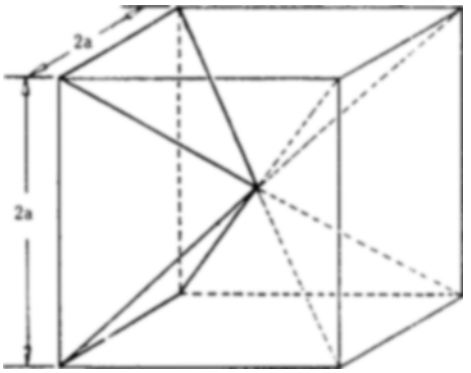

Fig. 1. Tetragonal pyramids in a cube.

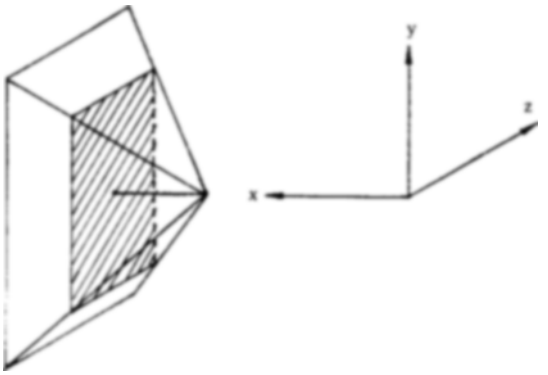

Fig. 2. A square plane, representing the ion exchange front.

2. The cubic model

The cubic model was developed for zeolite A powders which has cubic shape, based on the following assumptions:

1. Individual crystallites of zeolite NaA is well dispersed in a finite volume of a batch ion exchange solution.

2. The rate of ion exchange at the ion exchange site in zeolite cages is much faster than the diffusion of cations through cage pores.

3. The diffusivity of cations through zeolite cages is constant.

Since a cube is made of six identical tetragonal pyramids symmetrically located each other as shown in Fig. 1, the analysis was made based on a tetragonal pyramid rather than on a cube so that the three dimensional problem could be reduced to a one dimensional problem. Based on the second assumption above, the ion exchange front at a given time could be represented by a square plane in the pyramid parallel to the base plane, as shown in Fig. 2. Taking the apex of the pyramid as the origin of a rectangular coordinate system, the distance from the apex normal to the base plane is represented by the x-coordinate as in Fig. 2.

Now the diffusion equation through a square plane at $x = x$ is

$$\frac{\partial C_f^s}{\partial t} = \frac{1}{A(x)} \frac{\partial}{\partial x} \left[DA(x) \frac{\partial C_f^s}{\partial x} \right] \tag{2}$$

where A(x) is the area of the square at $x = x$ (i.e. $4x^2$) and C_f^s is the concentration of the ionic solution in the solid phase. The boundary condition at the external surface of a zeolite NaA crystallite is

$$V \frac{\partial C_f}{\partial t} = -4a^2 D \frac{\partial C_f}{\partial x} \quad @\ x = a,\ t \geq 0. \tag{3}$$

For zeolite NaA powders dispersed in a finite volume of well agitated cationic solution, the rate of cation transferred to the surface of a crystallite from the bulk of solution is equal to the rate of diffusion in the solid phase in the negative x direction,

$$-\left(\frac{V}{4a^2}\right) \frac{\partial C_f}{\partial t} = k_f (C_f - C_{fi}) = D \frac{\partial C_{fi}^s}{\partial x} \tag{4}$$

where C_{fi} and C_{fi}^s are the liquid and solid phase concentrations at the interface, respectively. At the moving front where the irreversible ion exchange is taking place,

$$S \frac{\partial x_o}{\partial t} = -D \frac{\partial C_f^s}{\partial x} \quad @\ x = x_o,\ t > 0 \tag{5}$$

where S is the surface concentration and x_o the location of the ion exchange front. The outside region of a crystallite, $x \geq x_o$, is in equilibrium with the local ionic concentration, whereas in the inside region, $x_o \geq x \geq 0$, there exists no ion exchange cations, i.e. $C_f^s = 0$.

Since the rate of ion exchange is assumed to be much faster than the speed of the front movement, a quasi-steady state could be assumed in the region between the external surface and the front. Thus, Eq.(2) could be expressed as follows,

$$C_f^s = C_{fi} \frac{a}{x} \left(\frac{x - x_o}{x - a} \right) \quad a \geq x \geq x_o. \tag{6}$$

Taking differential derivatives of Eq. (6) at the external surface, i.e. $x = a$, and substituting it into Eq. (4), we get

$$-\frac{V}{4a^2} \frac{\partial C_f}{\partial t} = \frac{x_o C_{fi} D}{a(a - x_o)} = k_f (C_f - C_{fi}). \tag{7}$$

Eliminating C_{fi} from Eq. (6),

$$V \frac{\partial C_f}{\partial t} = \frac{-4a^2 C_f}{\left(\frac{a}{D}\right)\left(\frac{a - x_o}{x_o}\right) + \frac{1}{k_f}}. \tag{8}$$

To get C_f as a function of t only, x_o in Eq. (8) now has to be eliminated. Combining Eqs. (3) and (5) and integrating over from x = a to x = x_o, we get

$$\frac{C_f}{C_{fo}} = 1 + \frac{4S}{3VC_{fo}} a^3 \left[\left(\frac{x_o}{a} \right)^3 - 1 \right]. \tag{9}$$

At the end point of ion exchange ($x_o = 0$), Eq. (9) becomes

$$\frac{C_{fe}}{C_{fo}} = 1 - \left(\frac{4S}{3VC_{fo}} \right) a^3 \tag{10}$$

where C_{fe} is the concentration of the bulk solution at equilibrium. Substituting Eq.(10) in Eq. (9), we have

$$\frac{C_f}{C_{fo}} = \frac{C_{fe}}{C_{fo}} + \left(\frac{x_o}{a} \right) \left(1 - \frac{C_{fe}}{C_{fo}} \right). \tag{11}$$

Now, taking $\phi = C_f/C_{fo}$ and $\phi_e = C_{fe}/C_{fo}$ Eq. (11) can be simplified as

$$\frac{x_o}{a} = \left(\frac{\phi - \phi_e}{1 - \phi_e} \right)^{1/3}. \tag{12}$$

Substituting Eq. (12) in Eq. (8), rearranging and integrating it becomes

$$\int_1^{\phi} \frac{1}{\phi} \left(\frac{1}{\left(\frac{\phi - \phi_e}{1 - \phi_e} \right)^{1/3}} - 1 \right) d\phi + \frac{D}{k_f a} \int_1^{\phi} \frac{d\phi}{\phi}$$

$$= - \frac{4aD}{V} \int_0^t dt \tag{13}$$

where V represents the volume of ion exchange solution per 1/6 of a cubic crystallite, or

$$V = \frac{1}{6} \frac{\rho_p}{w} (2a)^3 \tag{14}$$

where ρ_p is the density of zeolite crystallite and w the dosage of zeolite crystallites in the batch ion exchange solution.

Introducing a new function $F(\phi)$, defined by the following equation,

$$F(\phi) = \int_1^{\phi} \frac{1}{\phi} \left(\frac{1}{\left(\frac{\phi - \phi_e}{1 - \phi_e} \right)^{1/3}} - 1 \right) d\phi. \tag{15}$$

Eq. (13) can be expressed by the following simplified form,

$$\frac{F(\phi)}{\ln \phi} = \frac{D}{k_f a} + \frac{3wDt}{a^2 \rho_p \ln \phi}. \tag{16}$$

3. Comparison of cubic and spherical model equations

Although Eq. (16) for cubic particles is similar to Eq. (1) for spherical particles, the geometrical constants a and r should be correlated on the same volume basis. Since $V_{sphere} = 3\pi r^3/4$ and $V_{cube} = (2a)^3$, the corresponding radius of a sphere to a cube of the same volume is

$$3\pi r^3/4 = (2a)^3$$

$$r = 1.241a. \tag{17}$$

Therefore, in terms of the equivalent cube half size, a, Eq. (1) becomes

$$\frac{F(\phi)}{\ln \phi} = 0.806 \frac{D}{k_f a} + 1.949 \frac{wDt}{a^2 \rho_p \ln \phi} \tag{18}$$

Comparing Eqs. (16) and (18), we can see that the spherical model would give higher values of diffusivity than the cubic model when used in analysis of the same experimental data.

4. The transition model

The crystalline network of zeolite A is made of a cubic array of unit cells, each unit cell being interconnected to six other cells through six windows located on the surfaces of a cube [1]. Unit cells on the external surface of a zeolite A crystallite can be classified into three types based on the numbers of windows open to the surroundings as follows;

type 1 — those cells located at the corners of a cubic crystallite with three windows open to the surrounding,

type 2 — those cells on the edges with two windows open,

type 3 — those cells on the inside of each face plane of a cube with only one window open.

As ion exchange process begins, type 1 cells would admit exchanging cations faster than type 2 cells, and type 2 faster than type 1 because of the difference in the number of windows available for diffusion of cations. Also, as the ion exchange front moves inward, the size of the cube with fresh cells would continue to shrink, resulting in an increase in the fraction of type 1 cells and to a lesser degree type 2, compared to type 3, the fraction of which being shrunk steadily. This would cause a slow transition of the shape of ion exchange front from cubic initially to a round-edged cube, and eventually to a shape similar to a sphere. To show the change of the shape of the mass transfer front, a mass transfer to a cube at a constant surface concentration was solved analytically [6]. The resulting plot of isosteres at different contact time is shown for $\tau = 0.08$ and $Z = z/a = 0$ in Fig. 3.

It clearly shows the steady transition of the diffusion front from a square to a rounded shape in the two dimensional plot. The dotted line in the plot represents the boundary where the frontal shape start to

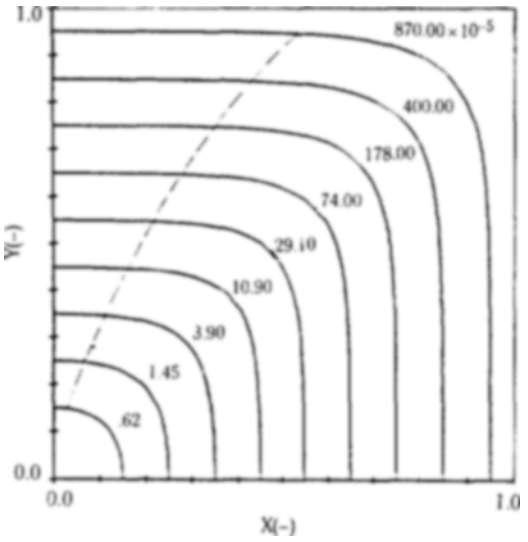

Fig. 3. Transition of diffusion front from cubic to spherical shape (γ = 0.08, Z = 0.00).

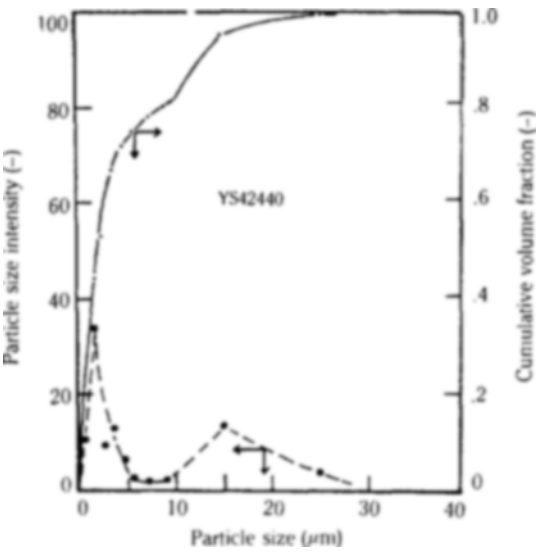

Fig. 4. Particle size distribution of zeolite NaA crystallites (before separation of aggregates).

deviate from straight line.

To take account of this phenomenon in the analysis of experimental ion exchange rates, the rate equations for cube and sphere are combined together in the following form,

$$f_T(\phi) = \frac{F(\phi)}{\ln \phi} = [1 - g(\theta)] f_C(\phi) + g(\theta) f_S(\phi) \quad (19)$$

where $f_T(\phi)$ represents the rate equation for the transition model, $f_C(\phi)$ for cubic and $f_S(\phi)$ for spherical model, respectively. $g(\theta)$ denotes the transition time function reflecting the fractional contribution of cubic model to the overall rate.

Substituting Eqs. (16) and (18) into Eq. (19), it becomes

$$\frac{F(\phi)}{\ln \phi} = [1 - 0.194 g(\theta)] \frac{D}{k_f a} + [3 - 1.051 g(\theta)] \frac{wDt}{a^2 \rho_p \ln \phi}. \quad (20)$$

The transition time function, $g(\theta)$, is related to the dotted line in Fig. 3 and could be found from experimental rate data.

EXPERIMENT

1. Synthesis of zeolite NaA crystallites

To study the effect of different crystallite size on the ion exchange rate, zeolite NaA samples were synthesized directly under different conditions. Samples of different crystallite size were obtained by changing the aging time which precedes the crystallization step [7]. The longer the aging time the smaller the crystallite size it becomes. However, all zeolite samples were reported to contain aggregates of crystallites to some extent [8-10]. The particle size distribution of a zeolite synthesis batch, shown in Fig. 4, confirms the existence of large aggregate particles, i.e. those above 10 μm.

To avoid errors which would be caused by the existence of these aggregates, zeolite samples were treated by a floatation method in water and large aggregate particles were removed before ion exchange experiments. Crystallite size of zeolite samples were analysed by SEM.

2. Pretreatment of zeolite

Zeolite NaA samples were pretreated in 0.1N NaCl solution for 24 hours and then stored in a desiccator. The result of chemical analysis of these zeolite samples are given in Table 1. Sodium content was determined by atomic absorption spectrometry and water, silicon and aluminum by standard gravimetric methods [11], and others by ICPA (inductively coupled plasma atomic emission spectrometry).

3. Measurement of ion exchange rate

The ion exchange reactor (1L volume) was filled with a $CaCl_2$ solution and a given amount of zeolite NaA sample was added into the reactor under rapid stirring. The change in Ca^{2+} ion concentration was continuously monitored by a selective ion analyser (Fisher model 750), attached with a calcium electrode or a divalent cation electrode. The equilibrium con-

Table 1. Analysis of zeolite NaA

Sample No.: YS40040-1		Sample No.: YS40440-1	
Component	Content (wt%)	Component	Content (wt%)
Al_2O_3	31.80	Al_2O_3	31.02
SiO_2	33.74	SiO_2	33.16
Na_2O	19.01	Na_2O	18.56
H_2O	15.17	H_2O	17.02
others*	0.28	others*	0.24
Si/Al	0.90	Si/Al	0.91
Na/Al	0.98	Na/Al	0.98

others* : CaO, Fe_2O_3, K_2O, MnO, TiO_2

Table 2. Particle size and size distribution of zeolite NaA crystallites (after separation of aggregates)

Sample No.	Mean cube size, 2μ (μm)	Standard deviation, 2σ (μm)	$s = \frac{\mu}{\sigma}$
YS40040-1	3.072	1.339	2.294
YS40440-1	1.210	0.385	3.143
YS40840-1	1.130	0.243	4.650
YS41240-1	0.947	0.197	4.807
YS42440-1	0.759	0.169	4.490

centration of the solution was analysed by an atomic absorption spectrophotometer.

RESULTS AND DISCUSSION

1. Crystallite size and its distribution

Mean particle size of zeolite NaA samples, measured by SEM, are summarized in Table 2. The first digit of the sample number in the table, 4, designates zeolite NaA, and the next two digits the aging time in hours and the last two the aging temperature in degree Celsius. The number 1 following the hyphen (-) means it was pretreated by a floatation method to separate large aggregates. Mean cube size, i.e. 2a, of synthesized zeolite samples ranges from around 0.8 μm to above 3 μm, depending on the aging time used.

2. Rate of ion exchange vs. particle size

Fig. 5 shows the rate of calcium exchange of various zeolite NaA samples before the separation of aggregates by floatation. Because of the existence of large aggregates in random fractions, it does not show any meaningful trends between the rate and the particle size. Fig. 6 shows the rate data of floated zeolite NaA samples and there exists a definite correlation between

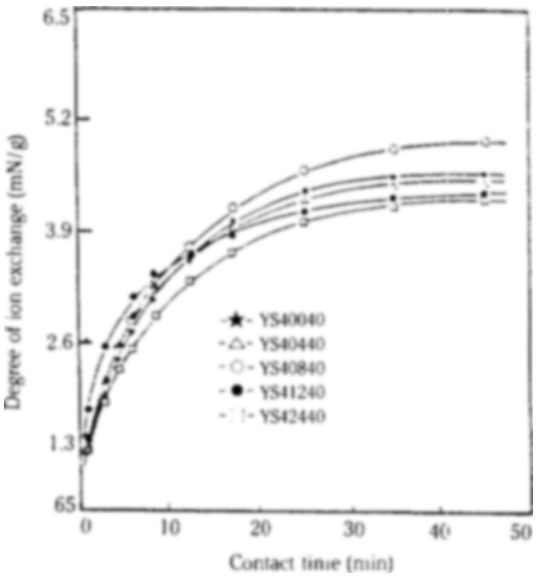

Fig. 5. Effect of crystallite size on Ca^{2+} ion exchange rate (before separation of aggregates, 108 ppm).

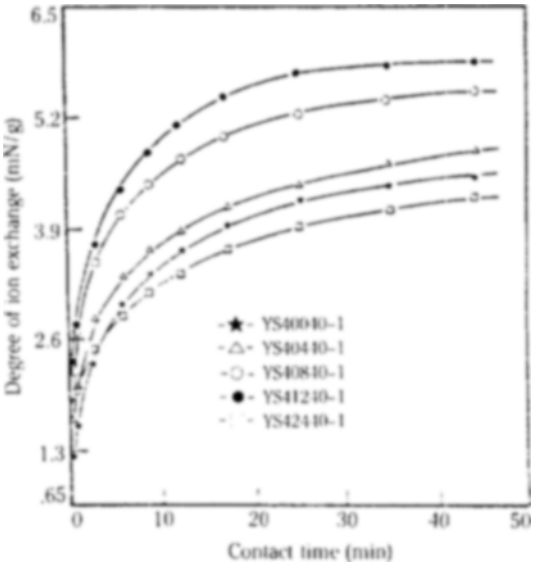

Fig. 6. Effect of crystallite size on Ca^{2+} ion exchange rate (after separation of aggregates, 108ppm).

the rate and the size, as expected, except for the sample YS42440-1. Although it has the smallest crystallite size, the rate is the slowest. It is quite possible that smaller aggregates of the small crystallites, i.e. in the range of 5 to 15 μm, could not have been completely separated from the sample by the simple floatation

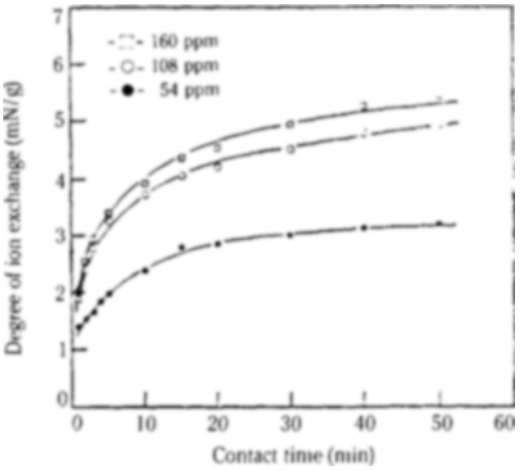

Fig. 7. Effect of initial fluid concentration on Ca^{2+} ion exchange rate, YS40440-1.

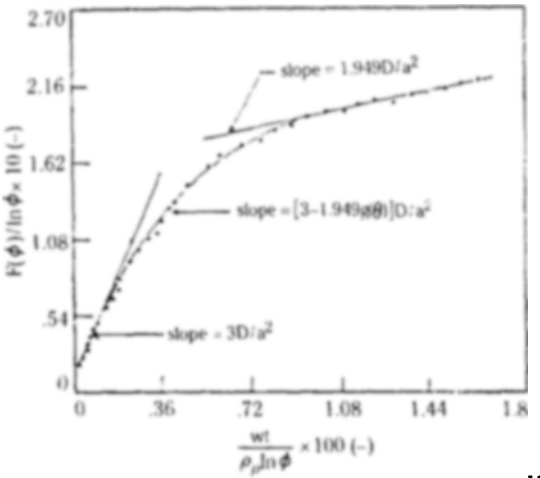

Fig. 8. Plot of ion exchange rate data, YS40040-1,108 ppm.

method. Fig. 7 shows the effect of the initial $CaCl_2$ concentration on the ion exchange rate.

3. Analysis of results by rate equations

Experimental results were plotted in the form of $F(\phi)/\ln\phi$ vs. $wt/\rho_p \ln\phi$ as shown in Fig. 8. Apparently the plot does not follow the linearity suggested by either the spherical or the cubic model equation. Therefore the resulting curve was analysed using the transition model equation. The slope of the curve at the beginning of the curve is interpreted to represent the cubic model, whereas the tangent to the curve at the end the spherical model. The intermediate region of the curve represents where both the cubic and the spherical model are contributing to the overall rate.

The intermediate portion of the curve was analysed

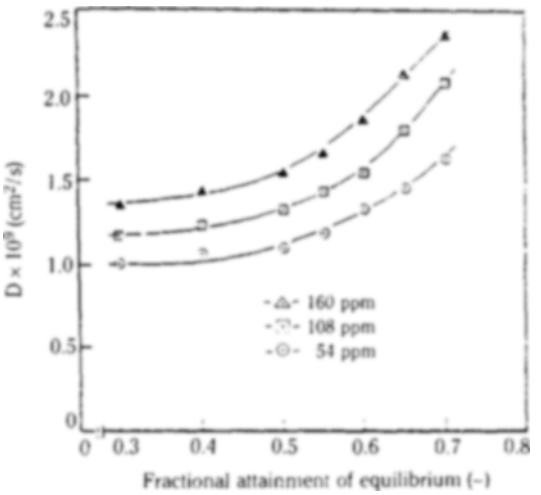

Fig. 9. Plot of effective diffusivity for Ca^{2+} ion by curve fitting method, YS40040-1.

using the transition model, Eq. (20). The slope and the intercept of the transition model are given by $[3\text{-}1.051\, g(\theta)]\, D/a^2$ and $[1\text{-}0.194 g(\theta)]\, D/k_f a$, respectively. Thus, if the film mass transfer coefficient, k_f, is known, the effective diffusivity, D, and the transition time function, $g(\theta)$, can be obtained from the experimental curve. The film coefficient could be estimated by the modified Frossling equation [12,13], given below.

$$N_{Sh} = 2.0 + 0.60\, N_{Re}^{1/2} N_{Sc}^{1/3} \quad (21)$$

The value of k_f employed in the computation ranges from 0.01 to 0.04 cm/s depending on the experimental conditions employed.

Effective pore diffusivity, D, of calcium ion in zeolite NaA crystallite was plotted against the fractional attainment of equilibrium, C_f^s/C_{fe}^s, in Fig. 9. It shows that the diffusivity increases as the degree of ion exchange increases. Since the calcium ion exchange of zeolite NaA increases the pore size of zeolite NaA from 4Å to 5Å, the increase in diffusivity with the degree of ion exchange is reasonable. Also, the transition from cubic to spherical shape would contribute to the increase in diffusivity. Fig. 10 shows a plot of effective diffusivity vs. crystallite size. Between the half size, a, of around 0.5 to 1.5 μm, the effective diffusivity seems to be independent of crystallite size at a given cationic concentration. Increase of cationic concentration, however, increases the diffusivity, in the range of concentration studied in this paper.

The low diffusivity of the sample of the smallest crystallite size, which was synthesized with the longest aging time, seems to indicate that the excessively long aging time would promote the formation of small aggregates which cannot readily be eliminated by a sim-

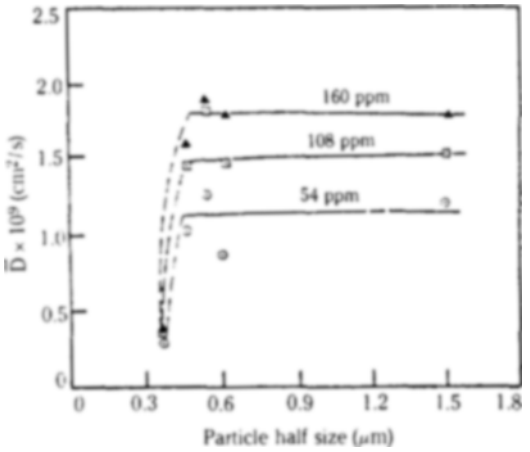

Fig. 10. Effect of particle size on effective diffusivity.

Table 3. Effective pore diffusivity, 5×10^9 (cm^2/s)

Sample \ Conc.	54 ppm	108 ppm	160 ppm
YS40040-1 (a = 1.503μm)	1.23	1.52	1.77
YS40440-1 (a = 0.605μm)	0.85	1.47	1.77
YS40840-1 (a = 0.565μm)	1.27	1.83	1.97
YS41240-1 (a = 0.474μm)	1.03	1.47	1.60
YS42440-1 (a = 0.380μm)	0.28	0.33	0.33

cf. $2.5 \times 10^{-11} - 2 \times 10^{-10}$ cm^2/s (from Ref. 14)
$1 \times 10^{-10} - 2.2 \times 10^{-10}$ cm^2/s (from Ref. 15).

ple floatation method. The small aggregates, if present in a significant amount, would results in a larger effective size than the size measured by SEM. Experimental values of effective diffusivity are summarized in Table 3.

Fig. 11 shows the plot of the transition time function, $g(\theta)$, vs. dimensionless time, $\theta = t/t_c$, obtained from the intermediate part of the rate curve. From these data points, representing various experimental conditions, the following transition time function was derived.

$$g(\theta) = 2.79\,\theta^{0.43} \tag{22}$$

The transition time function may be expressed in the following general form,

$$g(\theta) = \alpha\,\theta^{\beta} \tag{22a}$$

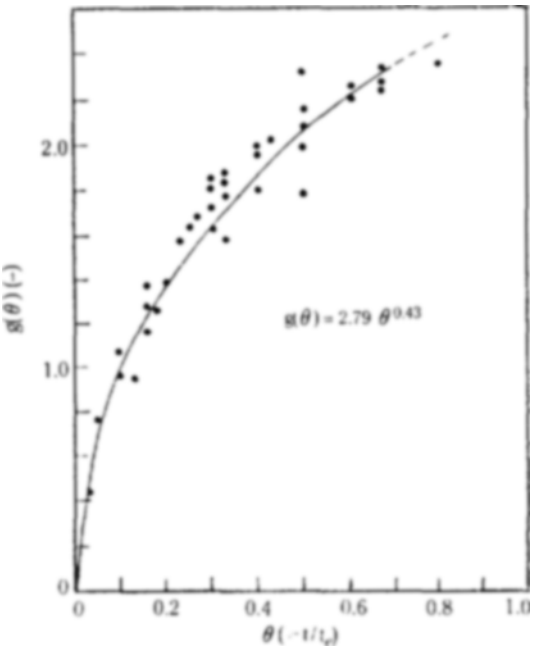

Fig. 11. Plot of transition vs. dimensionless ion exchange time.

where α and β are constants which depend on the ion exchange system.

CONCLUSION

The rate of calcium exchange of zeolite NaA powder of varying crystallite size was experimentally studied. The analyses of the experimental data by the spherical, the cubic and the transition models showed the followings:

1. Simple models of either the spherical or the cubic could not be satisfactorily applied to the ion exchange system studied.

2. The transition model combining the two simple models, which is represented by the following equation, could be applied to the ion exchange system studies quite satisfactorily.

$$f_T(\phi) = \frac{F(\phi)}{\ln \phi} = \frac{[1 - 0.194g(\theta)]D}{k_f a} + \frac{[3 - 1.054g(\theta)]wDt}{a^2 \rho_p \ln \phi}$$

where the transition time function, $g(\theta)$, represents the transition of ion exchange mechanism from initially cubic to spherical at the end. For the ion exchange system studied, the transition time function was found to be $g(\theta) = 2.79\,\theta^{0.43}$.

3. The effective pore diffusivity for calcium ion in zeolite NaA, calculated based on the transition model, were in the range of 10^{-10} to 10^{-9} cm^2/s.

NOMENCLATURE

a : cube half size, [cm]
C_f : liquid phase concentration, [mN/g]
C_f^* : liquid concentration in solid particle, [mN/g]
C_{fe} : liquid phase concentration at equilibrium, [mN/g]
C_{fi} : liquid phase concentration at interface, mN/g]
C_{fo} : initial liquid phase concentration, [mN/g]
D : effective pore diffusivity, [cm^2/s]
$g(\theta)$: transition time function, [-]
k_f : film mass transfer coefficient, [cm/s]
r : radius of spherical particle, [cm]
S : surface concentration, [mN/g]
t : time, [s]
t_e : equilibrium time, [s]
V : volume of solution per 1/6th of a cube particle, [cm^3]
w : zeolite dosage, [g/cm^3]
x : cube half size coordinate, [cm]

Greek Letters

ϕ : dimensionless liquid phase concentration, C_f/C_{fo}, [-]
ϕ_e : dimensionless liquid phase concentration at equilibrium, C_{fe}/C_{fo}, [-]
ρ_p : particle density, [g/cm^3]
θ : dimensionless ion exchange time, t/t_e, [-]
τ : dimensionless diffusion time, Dt/a^2, [-]
μ : mean cube half size, [cm]

REFERENCES

1. Breck, D.M.: "Zeolite Molecular Sieves", John Wiley & Sons, Inc., 83 (1974).
2. Barrer, R.M.: "Hydrothermal Chemistry of Zeolites", Academic Press (1982).
3. Crank, J.: "The Mathematics of Diffusion", Oxford Press (1979).
4. Digiano, F.A. and Weber, W.J.: *J. of Sanitary Eng. Div., Proc. of A.S.C.E.*, **98,** 1021 (1972).
5. Crank, J.: *Trans. Faraday Society*, **53,** 1083 (1957).
6. Carslaw, H.S. and Jaeger, J.C.: "Conduction of Heat in Solid", Oxford Press (1959).
7. Lee, H.: Proc. of 2nd ROC/ROK Joint Workshop on Catalysis, 53, UCL-ITRI, Taiwan (1984).
8. Dhank, B. and Sand, L.B.: *J. of Cat.*, **48,** 129 (1977).
9. Ciric, J.: *J. of Colloid & Interface Sci.*, **28,** 315 (1968).
10. Robert, F.G.: "Molecular Sieve Zeolite-I", Adv. in Chem. Ser., 101, ACS Press, 44 (1971).
11. Barrer, R.M. and Townsend, R.P.: *J. Chem. Soc., Faraday Trans.* 1, **22,** 661 (1976).
12. Frossling, N.: *Gerlands Beitr. Geophys.*, **52,** 170 (1938).
13. Ranz, W.E. and Marshall, W.R.: CEP, 48, 141-146, 173-180 (1952).
14. von Wolf, F., Danes, F. and Pilchowski, K.: *Z. Phys. Chemie, Leipzig*, **252,** 33 (1973).
15. van Bekkum, H., et al.: *Tenside Detergents*, **210,** 5 (1984).